

# BRAIN MRI $T_1$ -MAP AND $T_1$ -WEIGHTED IMAGE SEGMENTATION IN A VARIATIONAL FRAMEWORK

Ping-Feng Chen<sup>a</sup>, R. Grant Steen<sup>b</sup>, Anthony Yezzi<sup>c</sup>, and Hamid Krim<sup>a</sup>

<sup>a</sup>North Carolina State University, Department of Electrical and Computer Engineering,

<sup>b</sup>Medical Communications Consultants, LLC

<sup>c</sup>Georgia Institute of Technology, School of Electrical and Computer Engineering

Email: pchen@ncsu.edu

## ABSTRACT

In this paper we propose a constrained version of Mumford-Shah's [1] segmentation with an information-theoretic point of view [2] in order to devise a systematic procedure to segment brain MRI data for two modalities of parametric  $T_1$ -Map and  $T_1$ -weighted images in both 2-D and 3-D settings. The incorporation of a tuning weight in particular adds a probabilistic flavor to our segmentation method, and makes the three-tissue segmentation possible. Our method uses region based active contours which have proven to be robust. The method is validated by two real objects which were used to generate  $T_1$ -Maps and also by two simulated brains of  $T_1$ -weighted data from the BrainWeb [3] public database.

**Index Terms**— Active contour, Region-based active contour, Mumford-Shah,  $T_1$ -Map,  $T_1$ -weighted image

## 1. INTRODUCTION

Brain segmentation has been a popular research topic for a long time and numerous works have plunged into this study. Because manual tracing of the boundaries of tissues in the brain is labor intensive and unrealistic for large amount of data, an automatic or semiautomatic segmentation technique becomes very helpful for either visualization or diagnosis purposes. Different modalities, such as  $T_1$ -weighted,  $T_2$ -weighted, or PD (Proton Density) images, have been used for different segmentation methods.  $T_1$ -weighted images, because of their good contrast [4], have been widely tested for various segmentation methods [5, 6]. A parametric  $T_1$ -Map is an image of pure  $T_1$  (Spin Lattice Relaxation Time) value which is different from a  $T_1$ -weighted image. The relationship between  $T_1$  and several diseases, such as schizophrenia or sickle cell disease, has been studied [7], and  $T_1$  may be used as a possible indicator of pathology. The change of  $T_1$  values for certain voxels in the brain (i.e. the change from one tissue to another) over time, in particular, may be characterized as early indicators of possible diseases. Therefore, the segmentation of a parametric brain  $T_1$ -Map may highlight pathology unseen by other approaches.

Numerous works have studied the segmentation of cortical surfaces in the brain. The three tissues: white matter (WM), gray matter (GM), and cerebrospinal fluid (CSF) constitute the main parts in the brain. The goal is to find their respective boundaries. Different methods have been proposed to achieve this goal, and our method falls in the active contour category [6, 4]. It is an adaptive version of Mumford-Shah's model [1] to systematically segment different tissues in the brain.

The paper is organized as follows. In section 2 we state our proposed model, which has two adaptations to Mumford-Shah's original energy functional. In section 3 we illustrate our proposed systematic methods to segment a brain  $T_1$ -Map. In section 4 we show the segmentation results of  $T_1$ -Maps, and also for  $T_1$ -weighted data in the 3-D setting, to show the generality of our method, both with validations. At last in section 5 we conclude the paper.

## 2. PROPOSED MODEL FOR SEGMENTATION

As an alternative to looking for edge information such as the gradient, region-based active contours minimize energy functionals to detect homogeneous regions. We will use a modified Mumford-Shah [1] energy functional:

$$E(f_{R_{in}}, f_{R_{out}}, \vec{C}) = \sum_{i=in,out} \beta_i \int_{R_i} \left\{ (f_{R_i} - G(I))^2 + \nu \|\nabla f_{R_i}\|^2 \right\} dx + \alpha \oint_{\vec{C}} ds, \quad (1)$$

where  $f_{R_i}$  approximate a function  $G(\cdot)$  applied of the image  $I$  for region  $R_i$ ,  $i = in$  or  $out$ .  $f_{R_i}$  is smooth within each region  $R_i$ , but not across the boundaries;  $\vec{C}$  denotes the region boundaries, which is the *contour* of interest in this paper, and  $0 \leq \beta_i \leq 1$  are weights such that  $\beta_{in} + \beta_{out} = 1$ . By minimizing this functional we obtain a function  $f_{R_i}$  which is faithful to the image (first term) and smooth within each

region but not across the boundaries (second term), while penalizing excessive length of the boundaries (last term).

Two adaptations in Eq. (1) for the problem of interest constitute the novelty of the proposed technique. First is the function  $G(\cdot)$  applied on to image  $I$  instead of the image itself. The first is motivated by the work of Unal *et al.*[2]. Specifically, an information-theoretic approach for maximizing a probabilistic disparity measure, Jensen-Shannon (JS) divergence, was proposed. A constructed function  $G(\cdot)$  characterizes the property of the probability density function (PDF) of the image intensity such as skewness, kurtosis, all relative to a Gaussian. A proper choice of  $G(\cdot)$  will capture the statistical characteristics of the data and will hence achieve a good segmentation.

The second contribution is the introduction of a selective weight favoring erring towards one tissue type or another. The assigned weight  $\beta_{in(out)}$ , in essence provides a probabilistic assignment to the segmented regions. Enhancing the weight of the interior of the evolving contour,  $\beta_{in}$ , is tantamount to penalizing the degree of smoothness of the approximated function. This would yield smaller segmented regions which is likely to be more faithful to the image and of "purer" tissues.

As for the approximated function  $f_{R_{in(out)}}$ , we adopted a fast Mumford-Shah implementation proposed by Alvino *et al.*[8]. They use a linear combination of a set of basis functions to represent the approximated function. With their so-called *linear heat equation basis* and the change from  $I$  to  $G(I)$ , we have

$$f_{R_i} = \gamma_{1,i}G(I) + \gamma_{2,i}mean(G(I)), \quad (2)$$

where  $i = in$  and  $out$ ,  $mean(\cdot)$  is the average function, and the coefficients  $\gamma_{j,i}$ 's may be derived in a similar manner as outlined in [8].

Substituting Eq. (2) into Eq. (1) and using traditional variational calculus methods, the evolution of the curve may be derived as

$$\begin{aligned} \frac{\partial \vec{C}}{\partial t} = & \left\{ \beta_{out} \left[ (f_{R_{out}} - G(I))^2 + \nu \|\nabla f_{R_{out}}\|^2 \right] \right. \\ & \left. - \beta_{in} \left[ (f_{R_{in}} - G(I))^2 + \nu \|\nabla f_{R_{in}}\|^2 \right] \right\} \mathbf{N} \\ & - \alpha \kappa \mathbf{N}, \end{aligned} \quad (3)$$

where  $\kappa$  denotes the curvature of the contour  $\vec{C}$ ,  $t$  an artificial time parameter, and  $\mathbf{N}$  the outward normal of the contour.

### 3. SEGMENTATION OF A PARAMETRIC BRAIN T<sub>1</sub>-MAP

We assume a binary brain mask has been obtained to get rid of everything except for the three tissues, WM, GM, and CSF, in the brain. Notice that the curve evolution corresponding to the energy introduced in section 2 always results in a "binary segmentation", where we will have regions *inside* (foreground)

and *outside* (background) the contour(s). We cannot segment the three tissues at once. We may however tune the weights in penalizing the error between the data term and the approximated function (Eq. (1)) differently to segment one tissue at a time, analogous to "peeling an onion".

For ease of explanation we illustrate our T<sub>1</sub>-Map segmentation procedure for a *hard segmentation* of three tissues, and the probabilistic segmentation can be obtained by varying the weights around the value of the trained weight, which will be demonstrated in section 4. A T<sub>1</sub>-Map segmentation procedure consists of three steps, where the first two steps are to evolve the contours by minimizing the energy in Eq. (1) with different weights, and the third step is just a simple subtraction. The procedure is: 1) treat WM as the foreground, everything else as the background, and let  $\beta_{in}$  be the trained weight  $\beta_{in,WM}$  in Eq. (1) to segment WM in the interior region of the contour, 2) treat WM and GM as the foreground, CSF and everything else as the background, and let  $\beta_{in}$  be the trained weight  $\beta_{in,CSF}$  in Eq. (1) to obtain CSF in the exterior region of the curve filtered by the brain mask, and 3) GM is obtained by subtracting the whole brain by WM and CSF. This procedure is based on the anatomical observation that GM is enclosed by CSF and separates CSF from WM[4], such that we may peel off one layer at a time.

The choice of function  $G(I)$  in Eq. (1), which is chosen to better capture the statistical properties of the T<sub>1</sub>-Map, will be shown in section 4. The value of  $\beta_{in,WM}$  and  $\beta_{in,CSF}$  are determined through a training process. Suppose an expert's manual segmentation is regarded as the ground truth. If  $R_e$  denotes the segmentation region by the expert, and  $R_{\beta_{in}}$  denotes the segmentation region by the weight  $\beta_{in}$  with some fixed  $G(I)$ , for some tissue, then the value of  $\beta_{in,tissue}$  is determined by minimizing

$$\beta_{in,tissue} = \arg \min_{\beta_{in}} \left\{ 1 - \frac{|R_e \cap R_{\beta_{in}}|}{|R_{\beta_{in}}| + |R_e| - |R_e \cap R_{\beta_{in}}|} \right\}, \quad (4)$$

where  $|R|$  denotes the number of pixels in region  $R$ . The first term inside the bracket is *overlap metric* (OM)[6]. It is commonly used to validate the segmentation performance – the closer to 1 the better the performance.

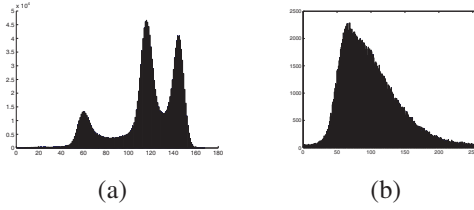
## 4. EXPERIMENTAL RESULTS

### 4.1. Segmentation of T<sub>1</sub>-Map

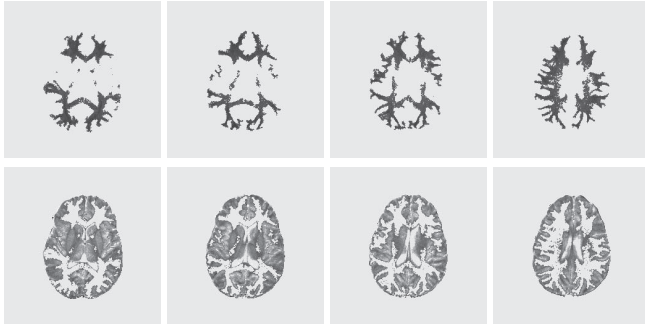
16 slices of T<sub>1</sub>-Maps are taken across different transverse planes, but only slices 5 through 15 are used for segmentation because they cover sufficient amounts of WM, GM and CSF and are least affected by RF (Radiofrequency)-inhomogeneity. The function  $G(I)$  introduced in Eq. (1) is empirically chosen as the cubic function  $I^3$ , which characterizes the *skewness* of a PDF. Moreover,  $\beta_{in,WM}$  and  $\beta_{in,CSF}$  are obtained by training according to Eq. (4) based on an expert's manual segmentation of one subject (*training subject*).

They are  $\beta_{in,WM} = 0.93$  and  $\beta_{in,CSF} = 0.53$  respectively. The same values are then applied on the other subject (*testing subject*). The segmentation of a T<sub>1</sub>-Map is obtained by evolving contours according to Eq. (3).

The curve evolution is based on gradient flow, and thus the final result depends on the initialization. A T<sub>1</sub>-Map does not enjoy the luxury of good contrast compared to a T<sub>1</sub>-weighted image. A T<sub>1</sub>-weighted image exhibits an intensity histogram such as that shown in Fig. 1(a), and one may carry out the spectral analysis to threshold the image as an initialization[6, 9]. T<sub>1</sub>-Map, on the other hand, does not have contrast as good as that shown in Fig. 1(b). We therefore initialize with either uniformly spaced squares or manually placed seeds (by mouse clicking and dragging on the image). Both methods give similar performance with manual seeding slightly better, and therefore we will show the results with manual seedings for T<sub>1</sub>-Map.



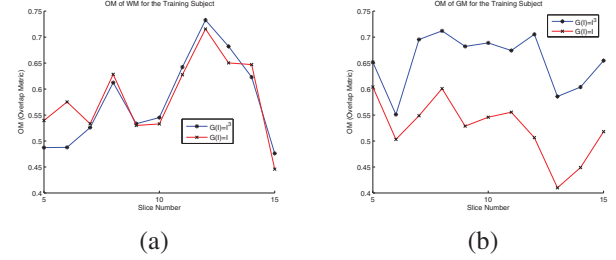
**Fig. 1.** Histogram of a (a) T<sub>1</sub>-weighted image and a (b) T<sub>1</sub>-Map.



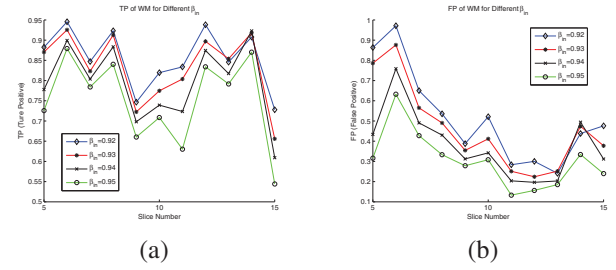
**Fig. 2.** Segmentation result of WM (first row) and GM (second row) for the testing subject at slice number 10 - 13.

Fig. 2 shows some selective segmentation results of WM and GM (CSF will be the brain mask subtracting WM and GM) for the testing subject. The validation of the results would require comparison with manual segmentations. The commonly examined metrics which determine the performance of a segmentation are TP (true positive), FP (false positive), and OM (overlap metric)[6, 4]. Fig. 3 shows two overlap metric curves (OM versus slice number) of WM and GM segmentation for the training subject (the testing subject exhibits a similar result). The first curve corresponds to the segmentation of T<sub>1</sub>-Maps with our tuned weights and the

cubic function  $G(I) = I^3$ , and the second corresponds to the segmentation with the function  $G(I) = I$  and tuned weights ( $\beta_{in,WM} = 0.9$  and  $\beta_{in,CSF} = 0.7$ ). The results show that with a different function  $G(I) = I$ , the performance of WM segmentation is comparable for these two functions, however there is a significant difference for CSF segmentation, thus affecting GM segmentation. The choice of cubic function  $I^3$  outperforms  $I$  tremendously for GM segmentation (as well as for CSF). It demonstrates that the former better characterizes the statistical properties of the data, in this case the skewness.



**Fig. 3.** Overlap metric of (a) WM and (b) GM segmentations for T<sub>1</sub>-Maps with cubic function  $G(I) = I^3$  and the data itself  $G(I) = I$ , both with tuned weights.



**Fig. 4.** (a) TP (True Positive) and (b) FP (False Positive) of WM segmentation for different weights  $\beta_{in}$ .

Fig. 4 shows TP and FP for WM segmentation with different weights  $\beta_{in}$  around the value of  $\beta_{in,WM}$ , to demonstrate the notion of our probabilistic segmentation.  $TP = \frac{|R_{\beta_{in}} \cap R_e|}{|R_e|}$ , and  $FP = \frac{|R_{\beta_{in}}| - |R_{\beta_{in}} \cap R_e|}{|R_e|}$ , where  $R_e$  and  $R_{\beta_{in}}$  are the expert-segmentations and those obtained using  $\beta_{in}$  respectively while  $|R|$  denotes the area of region  $R$ . When the weight increases, so does the penalty for the error between the data term and the approximated function (Eq. (1)). Therefore TP and FP decrease correspondingly, and vice versa.

#### 4.2. Segmentation of T<sub>1</sub>-weighted Images

In this section we would like to show the generality of our proposed segmentation method by testing it on a different modality in the 3-D setting. We apply it to a more often exploited modality: T<sub>1</sub>-weighted images. The same procedures are carried out as in section 3 except that now the images are

	WM	GM	CSF
TP(%)	89.8	91.8	85.1
FP(%)	6.9	12.5	9.6
OM	0.84	0.817	0.776

**Table 1.** Different validation metrics for the testing brain of  $T_1$ -weighted modality from BrainWeb.

collated into volumes and the active contour is replaced by an *active surface*. We test it on an open database accessible online- BrainWeb[3]. It is a simulated brain MRI database thus ground truth is already provided. We may therefore preprocess the data to filter out everything except for the three main tissues, WM, GM, and CSF, in the data.

We test our segmentation method on two (one as the training subject and the other as the testing subject) brain MRI datasets of  $T_1$ -weighted modality from BrainWeb. The images are of 1mm slice thickness, 3% noise level, and 20% RF intensity non-uniformity (INU) and the size of each subject is  $217 \times 181 \times 106$ . For this particular modality, since the contrast between different tissues is high, we carry out the histogram analysis and apply the threshold method similar to [6] for initialization. The function  $G(I)$  is still chosen as  $I^3$ , and  $\beta_{in,WM}$  and  $\beta_{in,CSF}$  are obtained by training as 0.3 and 0.2 respectively. The validation metrics for the testing subject are shown in Table 1. The results show that it achieves a high performance of OM around 0.8 for three tissues. Fig. 5 shows the segmentation results for the testing brain.

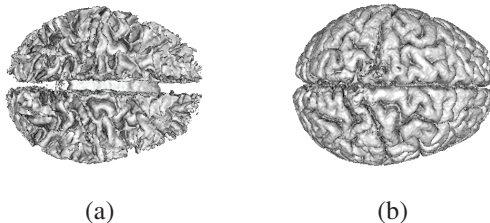


**Fig. 5.** 3-D segmentation results of (a) WM and (b) GM for the brain MRI  $T_1$ -weighted data from BrainWeb.

## 5. CONCLUSION

In conclusion, we propose an adapted Mumford-Shah type energy functional for segmentation. The two adaptations: 1) a function  $G(I)$  is able to better characterize the statistical properties of the data to achieve better segmentation results, and 2) the tuning weights  $\beta_{in(out)}$  are able to segment the brain tissues in a probabilistic fashion and achieve three-tissue segmentation. The method is validated both for  $T_1$ -Maps and  $T_1$ -weighted images, in both 2-D and 3-D settings, and the results show high performance with our method.

## 6. REFERENCES

- [1] David Mumford and Jayant Shah, "Optimal approximations by piecewise smooth functions and associated variational problems," *Comm. Pure Appl. Math*, vol. 42, 1989.
- [2] Gozde Unal, Anthony Yezzi, and Hamid Krim, "Information-theoretic active polygons for unsupervised texture segmentation," *International Journal of Computer Vision*, vol. 62, pp. 199–220, 2005.
- [3] BrwainWeb, "Mcconnell brain imaging center, montreal neurological institute," <http://www.bic.mni.mcgill.ca/brainweb/>.
- [4] Xiaolan Zeng, L.H. Staib, R.T. Schultz, and J.S. Duncan, "Segmentation and measurement of the cortex from 3-d mr images using coupled-surfaces propagation," *Medical Imaging, IEEE Transactions on*, vol. 18, no. 10, pp. 927–937, Oct. 1999.
- [5] C. Xu, D.L. Pham, M.E. Rettmann, D.N. Yu, and J.L. Prince, "Reconstruction of the human cerebral cortex from magnetic resonance images," *Medical Imaging, IEEE Transactions on*, vol. 18, no. 6, pp. 467–480, June 1999.
- [6] Hua Li, Anthony Yezzi, and Laurent D. Cohen, "Fast 3d brain segmentation using dual-front active contours with optional user-interaction," *Computer Vision for Biomedical Image Applications*, pp. 335–345, 2005.
- [7] R. Grant Steen, Courtney Mull, Robert McClure, Robert M. Hamer, and Jeffrey A. Lieberman, "Brain volume in first-episode schizophrenia: Systematic review and meta-analysis of magnetic resonance imaging studies," *The British Journal of Psychiatry*, vol. 188, no. 6, pp. 510–518, 2006.
- [8] Christopher V. Alvino and Anthony J. Yezzi, "Fast mumford-shah segmentation using image scale space bases," 2007, vol. 6498, p. 64980F, SPIE.
- [9] Zu Y. Shan, Guang H. Yue, and Jing Z. Liu, "Automated histogram-based brain segmentation in  $T_1$ -weighted three-dimensional magnetic resonance head images," *NeuroImageVolume*, vol. 17, no. 3, pp. 1587–1598, 2002.